Mechanistic Modeling of Broth Temperature in Outdoor Photobioreactors

QUENTIN BÉCHET,[†] ANDY SHILTON,[†] OLIVER B. FRINGER,[‡] RAUL MUÑOZ,[∥] AND BENOIT GUIEYSSE*[,†,§]

School of Engineering and Advanced Technology, Massey University, Private Bag 11 222, Palmerston North 4442, New Zealand, Environmental Fluid Mechanics Laboratory, Stanford University, Stanford, California 94305-4020, School of Civil and Environmental Engineering, Nanyang Technological University, Singapore 639798, Singapore, and Department of Chemical Engineering and Environmental Technology, Valladolid University, Paseo del Prado de la Magdalena, s/n, Valladolid, Spain

Received October 21, 2009. Revised manuscript received January 23, 2010. Accepted February 3, 2010.

This study presents the first mechanistic model describing broth temperature in column photobioreactors as a function of static (location, reactor geometry) and dynamic (light irradiance, air temperature, wind velocity) parameters. Based on a heat balance on the liquid phase the model predicted temperature in a pneumatically agitated column photobioreactor (1 m^2 illuminated area, 0.19 m internal diameter, 50 L gas-free cultivation broth) operated outdoor in Singapore to an accuracy of 2.4 °C at the 95% confidence interval over the entire data set used (104 measurements from 7 different batches). Solar radiation (0 to 200 W) and air convection (−30 to 50 W) were the main contributors to broth temperature change. The model predicted broth temperature above 40 °C will be reached during summer months in the same photobioreactor operated in California, a value well over the maximum temperature tolerated by most commercial algae species. Accordingly, 18 000 and 5500 GJ $year^{-1}$ ha^{-1} of heat energy must be removed to maintain broth temperature at or below 25 and 35 °C, respectively, assuming a reactor density of one reactor per square meter. Clearly, the significant issue of temperature control must be addressed when evaluating the technical feasibility, costs, and sustainability of large-scale algae production.

Introduction

Despite the considerable investment made in algae biofuel research in recent years (*1*), the feasibility and sustainability of full-scale mass algae cultivation remain highly debated because of significant biological limitations and scaling-up issues (*2*–*7*). Processes for algae cultivation are normally classified as photobioreactors or open ponds (*8*–*10*). Typically, photobioreactors support higher photosynthetic efficiencies, and therefore biomass productivities, than ponds whereas open ponds are more economical to build and operate (*3*, *8*). Because most of the sunlight reaching the culture is converted into heat, broth temperature can easily reach 40 °C in photobioreactors, a value well over the maximum temperature tolerated by most commercial algae species (*10*). In addition, each algae species operates at its maximum photosynthetic efficiency at an optimal temperature (*11*). Optimizing algal production would therefore require maintenance of broth temperature at its optimum value (*12*). Thus, to be able to predict algal productivity and process economics, we must understand how broth temperature is affected by environmental and process parameters.

This study presents the first fully mechanistic model describing broth temperature in column photobioreactor as a function of static (location, reactor geometry) and dynamic (light irradiance, air temperature, wind velocity) parameters. The model was validated against experimental broth temperature data from a pneumatically agitated column algal photobioreactor operated outdoor in Singapore. Broth temperature changes in a similar photobioreactor located in California were simulated to estimate the annual heat energy that must be removed to maintain the broth temperature below a certain value.

Materials and Methods

Modeling Approach. The photobioreactor broth was assumed completely mixed (all physical properties of the broth were considered uniform). In addition, as the algae dried weight (DW) and nutrient concentrations are generally very low (of the order of 1 g L^{-1}), every solution property (i.e., density, heat capacity, emissivity, etc.) was taken equal to that of water at standard temperature and pressure. For simplicity, every radiating body was considered as a gray-diffuse surface (e.g., its radiative properties do not depend on the wavelength or on the angle of the radiation).

The ground surface and the solution inside the reactor were considered opaque (absorptivity = emissivity). Considering the reactor broth as opaque restricts the model validity to light-limiting conditions. However, light-limited conditions would indeed be expected because (1) it is economically unsound to cultivate algae under nonlight-limiting conditions in large systems; and (2) light-limiting conditions occur at low algae densities in full scale photobioreactors (0.05 g DW/L in our system). The fraction of solar radiation used by algae to carry out photosynthesis (typically less than 4% of total solar radiation (*8*)) and microbial heat release (due to decay) were neglected in the heat balance. The wall surface was assumed to be a partly transparent gray-diffuse body and its transmittance τ was therefore defined as the ratio of the outgoing radiation over the incoming radiation. The fraction of radiation that does not penetrate the plastic wall was assumed reflected; there was therefore no absorption by the wall. Consequently, the emissivity of the wall was negligible and no radiation from the wall was considered. The reactor wall temperature was considered uniform and equal to the solution temperature because convection from the air to the plastic wall is negligible in comparison to the convection from the broth to the plastic wall. Other specific assumptions are described in the following section.

A heat balance analysis fo the liquid solution in the reactor (S1 in Supporting Information) yields

$$\rho_w V_r C p_w \frac{dT_r}{dt} = Q_{ra,r} + Q_{ra,d} + Q_{ra,D} + Q_{re,s} + Q_{ra,a} + Q_{re,a} + Q_{ra,g} + Q_c + Q_{ev} + Q_b + Q_{cond} \quad (1)$$

* Corresponding author phone: +64 6 350 5841; fax: +64 6 350 5604; e-mail: B.J.Guieysse@massey.ac.nz.
[†] Massey University.
[‡] Stanford University.
[∥] Valladolid University.
[§] Nanyang Technological University.

10.1021/es903214u
Published on Web 02/23/2010

where T_r is the reactor broth temperature (K); ρ_w and Cp_w are the density (kg m^{-3}) and the specific heat capacity (J kg^{-1} K^{-1}) of water, respectively; V_r *is* the volume of the broth (m^3); $Q_{ra,r}$ is the radiation from the reactor itself (W); $Q_{ra,D}$ is the direct solar radiation (W); $Q_{ra,d}$ is the diffuse solar radiation (W); $Q_{re,s}$ is the solar radiation reflected from the ground (W); $Q_{ra,a}$ is the radiation from the air surrounding the reactor (W); $Q_{re,a}$ is the air radiation reflected from the ground (W); $Q_{ra,g}$ is the radiation from the ground (W); Q_c is the convective flux (W); Q_{ev} is the evaporation flux (W); Q_b is heat flux into air bubbles (W); and Q_{cond} is the conductive flux with the ground surface at the base surface (W). In eq 1, the heat capacity of the plastic wall (in J K^{-1}) was neglected in the left-hand term because it is negligible compared with the heat capacity of the broth.

Radiation from the Reactor. As water radiates heat over the entire reactor surface, the radiation from the liquid phase based on the Stefan−Boltzmann's fourth power radiation law was expressed as (*13*)

$$Q_{ra,r} = -\sigma\tau\varepsilon_r(\pi R_r^2 + 2\pi R_r L_r)T_r^4 \quad (2)$$

where σ is the Stefan−Boltzmann constant (W m^{-2} K^{-4}); τ is the reactor wall transmittance (−); ε_r is the emissivity of the liquid phase (0.97 is used and is a common value for water); R_r is the reactor radius (m); L_r is the reactor height (water level, in m); and T_r is the reactor temperature (K).

Direct Solar Radiation. The heat flux arising from the direct solar radiation reaching the top of the reactor can be expressed as

$$Q_{ra,D,top} = \varepsilon_r\tau H_D\pi R_r^2 \quad (3)$$

where H_D (W m^{-2}) is the intensity of the direct solar radiation reaching the ground surface in the vertical direction.

The heat flux reaching the lateral surface of the water column $Q_{ra,D,lat}$ is

$$Q_{ra,D,lat} = \varepsilon_r\tau H_D \tan\theta_z 2R_r L_r \quad (4)$$

where θ_z (rad) is the angle between a vector normal to the ground surface and the sun direction (S2 in SI).

The total direct solar flux $Q_{ra,D}$ can then be expressed as

$$Q_{ra,D} = (Q_{ra,D,top} + Q_{ra,D,lat})f(t) \quad (5)$$

where $f(t)$ is a "shading" function set to 0 when the reactor is not exposed to the Sun and set to 1 otherwise. This function is used when environmental elements (such as buildings, vegetation, etc.) hide the reactor from the sun rays during the day (different shading functions for different surfaces can be used if needed).

The angle between a vector normal to the ground surface and the sun direction, θ_z, is a function of the latitude φ (rad), the solar declination δ (rad) and the solar hour and is expressed as (*14*) (S3)

$$\cos(\theta_z) = \sin\varphi\sin\delta + \cos\varphi\cos\delta\cos\omega \quad (6)$$

where ω is the radial position of the reactor in a geocentric model (rad). ω varies linearly in time from $-\omega_s$ to ω_s ($-\omega_s$ at sunrise and ω_s at sunset), where

$$\cos\ \omega_s = -\tan\delta \times \tan\varphi \quad (7)$$

The solar declination can be calculated as function of the day of the year, N, as (*14*)

$$\delta = 23.35\frac{2\pi}{360}\sin\left(2\pi\frac{284 + N}{365}\right) \quad (8)$$

In most cases, including the present study, total solar irradiance (diffuse plus direct) H_g (W m^{-2}) reaching the ground surface in the vertical direction was experimentally measured. Therefore, the direct and diffuse solar irradiance at the ground level H_D and H_d (W m^{-2}) can be expressed as a function of H_g as

$$H_D = (1 - K_d)H_g \quad (9a)$$

and

$$H_d = K_d H_g \quad (9b)$$

Here, K_d (−) is the fraction of diffuse radiation reaching the ground surface. K_d typically ranges from 0.1 to 0.3 (*14*).

Diffuse Solar Radiation. Diffuse radiation is emitted equally in all space directions and is independent of θ_z. It can be expressed as

$$Q_{ra,d} = \tau\varepsilon_r(\pi R_r^2 + 2\pi R_r L_r)H_d \quad (10)$$

Reflected Solar Radiation. Because the ground surface is considered diffuse, it reflects direct and diffuse solar radiation homogeneously in every direction. The reflectivity of the ground r_g (−) can then be defined as the ratio of the reflected flux over the incoming flux. In addition, as the ground is considered opaque, radiation theory (*13*) gives

$$r_g = 1 - \varepsilon_g \quad (11)$$

where ε_g is the ground surface emissivity. Knowing that H_g is the intensity of the solar flux, the total intensity reflected by the ground integrated over all directions is

$$Q_{re,s,tot} = r_g H_g \quad (12)$$

The fraction of this flux reaching the lateral surface of the reactor can be expressed as

$$Q_{re,s} = \tau r_g \varepsilon_r H_g S_g \quad (13)$$

where $f_{g,lat}$ (−) is the form factor from this surface to the ground and S_g is the ground surface reflecting sunlight (m^2). Applying the form-factor theory gives (*13*)

$$S_g f_{g,lat} = S_{r,lat} f_{lat,g} \quad (14)$$

where $S_{r,lat}$ is the lateral surface of the reactor (m^2) and $f_{lat,g}$ the form factor from the lateral surface to the ground (−). Because the ground surface is assumed to be infinitely large, one-half of the lateral surface can be exposed and $f_{lat,g}$ equals one-half. This yields

$$Q_{re,s} = \tau(1 - \varepsilon_g)\varepsilon_r H_g \pi R_r L_r f(t) \quad (15)$$

Air Radiation. According to the Stefan−Boltzman's fourth power law, the radiative flux (in W m^{-2}) generated by air at a temperature of T_a (K) is given by

$$Q_a = \varepsilon_a\sigma T_a^4 \quad (16)$$

Air radiates on the top surface of the reactor (flux $Q_{ra,a,top}$, in W) and on its lateral surface (flux $Q_{ra,a,lat}$, in W). Using the form-factor theory, these fluxes can be expressed as (*13*)

$$Q_{ra,a,top} = \tau\varepsilon_r Q_a S_{a,top} f_{a,top} \quad (17a)$$

and

$$Q_{ra,a,lat} = \tau\varepsilon_r Q_a S_{a,lat} f_{a,lat} \quad (17b)$$

where $S_{a,top}$ and $S_{a,lat}$ are the air surfaces "seen" by the top surface and the lateral surface (m^2) and $f_{a,top}$ and $f_{a,lat}$ the corresponding form factors equal to one and one-half, respectively. Using the form factor theory, the final expression for the flux $Q_{ra,a}$ is expressed as:

$$Q_{ra,a} = \tau\varepsilon_r\varepsilon_a\sigma T_a^4(\pi R_r^2 + \pi R_r L_r) \quad (18)$$

Reflection of Air Radiation on the Ground Surface. Because the ground surface is exposed to air radiation and is assumed to be gray-diffuse with the reflectivity coefficient r_g, a fraction of the heat flux reaching the ground is reflected on the lateral surface of the reactor. The heat flux $Q_{a\text{-}g}$ (W) radiated from the air reaching the ground surface is

$$Q_{a-g} = \varepsilon_a \sigma T_a^4 S_g \tag{19}$$

where S_g is the ground surface considered (m^2). The fraction of this flux reflected onto the water column lateral surface is

$$Q_{re,a} = r_g Q_{a-g} f_{g,lat} \tag{20}$$

Again, from the form factor theory, this formula can be simplified as

$$Q_{re,a} = \tau \varepsilon_r r_g \varepsilon_a \sigma T_a^4 \pi R_r L_r \tag{21}$$

Radiation from the Ground. As ground surface is exposed to the sun and air radiation, its temperature T_g (K) can reach relatively high values and the ground can radiate back to its environment. The ground surface was assumed to be thin and at a uniform temperature T_g (S4). The fraction of ground radiation reaching the reactor lateral surface can be expressed as

$$Q_{ra,g} = \tau \varepsilon_r \varepsilon_g \sigma T_g^4 S_{g,lat} f_{g-lat} \tag{22}$$

Again, the form factor theory yields

$$Q_{ra,g} = \tau \varepsilon_r \varepsilon_g \sigma T_g^4 \pi L_r R_r \tag{23}$$

Convection. Assuming that the temperature of the air in the bubbles reaching the top surface is at the reactor temperature T_r, there is no convection at the top surface. Therefore, the convection flux Q_c (W) on the wall lateral surface is (*15*)

$$Q_c = h_{co,lat}(T_a - T_r) 2\pi R_r L_r \tag{24}$$

where $h_{co,lat}$ ($W \cdot m^{-2} \cdot K^{-1}$) is the convection coefficient between the lateral surface and the air. Natural (no wind) and forced (wind) convection must be considered. The coefficient for natural convection can be expressed as (*15*)

$$h_{co,lat} = \frac{\lambda_a}{L_r}\left(0.825 + \frac{0.387 \mathrm{Ra}_{Lr}^{1/6}}{\left(1 + \left(\frac{0.492}{\mathrm{Pr}}\right)^{9/16}\right)^{8/27}}\right)^2 \tag{25}$$

where Pr is the Prandtl number for air (0.7 at 25 °C), λ_a is the air thermal conductivity ($W\,m^{-1}\,K^{-1}$), and Ra_{Lr} is the Rayleigh number expressed for L_r (−) as:

$$\mathrm{Ra}_{Lr} = \frac{g|T_r - T_a|L_r^3}{a_a \nu_a T_a} \tag{26}$$

where g is the gravity constant ($m\,s^{-2}$); ν_a is the air kinematics viscosity ($m^2\,s^{-1}$) and a_a is the air diffusivity ($m^2\,s^{-1}$).

The convection coefficient for forced convection can be calculated as (*15*)

$$h_{co,lat} = \frac{\lambda_a}{2R_r}\left(0.3 + \frac{0.62 \mathrm{Re}_{2Rr}^{0.5} \mathrm{Pr}^{1/3}}{\left(1 + \left(\frac{0.4}{\mathrm{Pr}}\right)^{2/3}\right)^{1/4}}\right)\left(1 + \left(\frac{\mathrm{Re}_{2Rr}}{282,000}\right)^{5/8}\right)^{4/5} \tag{27}$$

where Re_{2Rr} is the Reynolds number (−) expressed for the diameter of the reactor as

$$\mathrm{Re}_{2Rr} = \frac{\rho_a 2R_r \nu_w}{\mu_a} \tag{28}$$

where ρ_a is the air density, ν_w is the wind velocity, and μ_a is the air viscosity.

Evaporation. In this model, we assume the air leaving the reactor is saturated in water and at the reactor temperature. There is therefore no evaporation at the top surface of the liquid and the evaporative flux Q_{ev} can be expressed as

$$Q_{ev} = -(1 - RH) X_a F_b L_w \tag{29}$$

where RH is the incoming (i.e., ambient) air relative humidity (unitless) X_a is the concentration of water in saturated air (kg water m^{-3} air), F_b is the bubble flow rate ($m^3 \cdot s^{-1}$), and L_w is the water latent heat content ($J\,kg^{-1}$).

Cooling by Air Bubbling. As previously mentioned, air bubbles were assumed to reach thermal equilibrium with water before they reach the reactor top surface. The heat flux induced by bubbles can then be expressed as

$$Q_b = -Cp_a(T_r - T_a)\rho_a F_b \tag{30}$$

where Cp_a is the air specific capacity ($J\,kg^{-1}\,K^{-1}$) and ρ_a is the air density ($kg\,m^{-3}$).

Conduction. Using Fourier's law, the conductive flux between the liquid phase and the ground can be expressed as

$$Q_{cond} = -k_{wall}\frac{T_r - T_g}{l_{wall}}\pi R_r^2 \tag{31}$$

where k_{wall} is the wall conductivity ($W\,m^{-1}\,K^{-1}$) and l_{wall} is the wall thickness (m).

Validation. Experimental broth temperature data for validation of the model were obtained from a parallel study on *Chlorella sorokiniana* productivity in a column photobioreactor conducted in Singapore. A transparent acrylic cylindrical tank (2 m height × 0.19 m diameter) containing 50 L of gas-free cultivation broth was used as the pilot column photobioreactor. CO_2-enriched air (2−3%) was continuously bubbled at a rate of approximately 1.2 L min^{-1}; the corresponding working (gas bubbles + liquid) and overall volumes (gas bubbles + liquid + headspace) being 51.0 and 56.7 L, respectively. A multiprobe sensor (CyberScan PD650, Eutech, Thermo Fischer) was used for monitoring broth temperature. A complete description of reactor operation and monitoring is provided in S5. Meteorological data (air temperature, solar irradiance in $W\,m^{-2}$, wind speed, and air moisture) were obtained from a Vantage Pro II weather station (Davis Instrument, Hayward, CA) located on a building roof 200 m away from the photobioreactor. Data were recorded at 5 min intervals and are publicly available (*16*). In total, 7 batch experiments were conducted between August 20 and September 17, 2008 and 104 broth temperature measurements were made. Daily volumetric and algae areal productivities averaged 0.20 ± 0.04 g DW/L-d and 10 ± 2 g DW/m^2-d, respectively; algae concentration averaged 0.38 ± 0.05 g/L.

Computations. The equations described above were computationally integrated in time using the software MATLAB (The MathWorks, Natick, MA). A first-order forward Euler algorithm was chosen for its simplicity and the time step size was set to 100 s. Assuming the broth was at thermal equilibrium on the first morning of a batch study at 7 a.m., the initial temperature was taken equal to the air temperature at this time. Meteorological data (solar irradiance, air temperature, and wind velocity) collected every 5 min (*16*) were linearly extrapolated over the entire time interval and used for model validation. The meteorological data of 5 consecutive days during each climatic season (January 25−29, 2009; April 25−29, 2009; July 23−27, 2009; and October 25−29, 2008) at Merced, CA, were obtained from ref *17* and used for simulations. Selected values of physical parameters

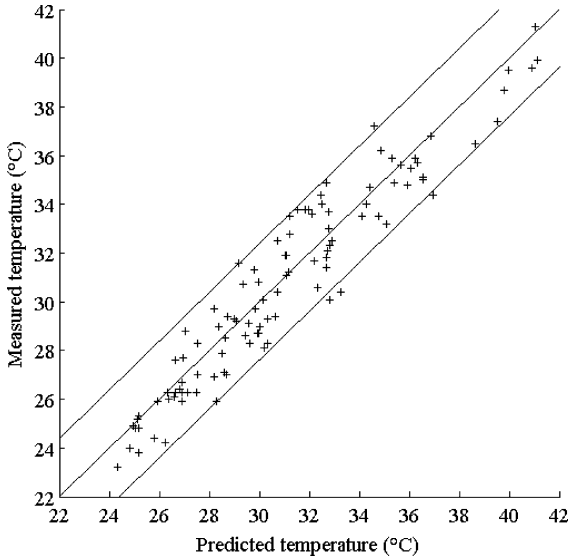

FIGURE 1. Comparison of experimental and predicted temperatures inside a column photobioreactor during outdoor cultivation in Singapore.

are shown in S6. Acuracy was defined as the maximum error between experimental and predicted data at the 95% confidence interval ($n = 104$, no experimental data were excluded).

Results and Discussion

Accuracy of Temperature Prediction. The model predicted the temperature of the culture broth of a photobioreactor operated in Singapore with an accuracy of 2.4 °C (Figure 1). The homogeneous distribution of error suggests the model does not systematically overestimate or underestimate temperatures over the range measured (23−41 °C). The accuracy of the temperature model is further illustrated by the 12-h (Figure 2) and 5-d (S7) predicted versus recorded temperature profiles during typical operation. In consequence, the assumptions made to simplify modeling can be considered as acceptable (a detailed discussion on these assumptions can be found in S8).

Uncertainty was introduced when fixing certain model parameters listed in S6 and when assuming other parameters were constant during operation (for example, wall transmittance can decrease due to dust and algae attachment). A sensitivity analysis was therefore conducted to quantify how varying these parameters would impact the model accuracy. For each parameter, the range of values acceptable to maintain the validation accuracy at 3 °C is shown in Table 1. For instance, it was demonstrated that wind velocity can be measured with an accuracy of 0.2 m s^{-1} against 1 °C for the air temperature and 8% for solar irradiance. By comparison, accuracies of weather station sensors were 0.1 m s^{-1} for the wind velocity, 5% for the solar irradiance, and 0.5 °C for the air temperature.

The sensitivity of time steps was evaluated to determine the frequency of climatic data collection required. It was found that in order to maintain accuracy within 3 °C, light irradiance data must be provided every hour whereas wind velocity and air temperature need to be supplied only every 4 and 8 h, respectively. When all three parameters were monitored every hour, the error was still lower than 3 °C (2.5 °C). This is significant for the use of the model as climatic data is often available on an hourly basis. By comparison, the model was able to predict temperature with an accuracy of 4.2 °C when 12 h-averaged climatic data were used (S9).

Five fluxes typically dominate the heat balance (Figure 3): radiation from the air, radiation from the ground, radiation from the reactor, solar radiation (including direct, diffuse, and reflected radiations), and convection. Evaporation from the top surface, cooling by bubbling, and conduction to the soil were not significant (<10 W). The positive heat fluxes from ground radiation (180−220 W) and air radiation (180−220 W) are within the same range as radiation losses from the reactor (−360 to −440 W). These ground, air, and reactor radiations fluxes are relatively constant (±10%) with respect to time because their proportionality to temperature is to the fourth power (the ground surface, the air, and the reactor temperatures fluctuated within less than 10% when expressed in K). Thus, changes in the reactor broth tem-

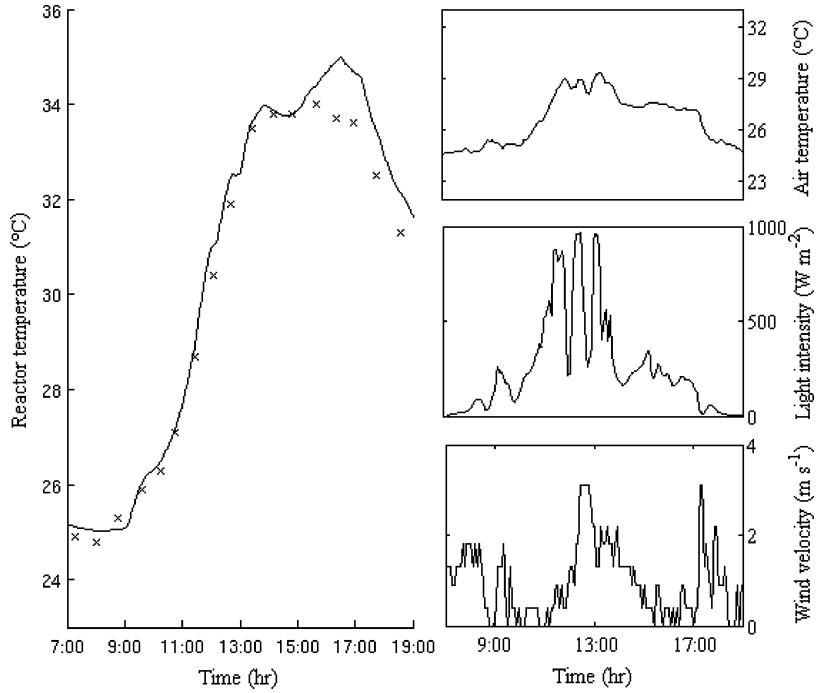

FIGURE 2. Change in experimental (crosses) and predicted (plain line) temperature inside a column photobioreactor on August 22, 2008 during outdoor operation in Singapore. Meteorological data are shown on the right.

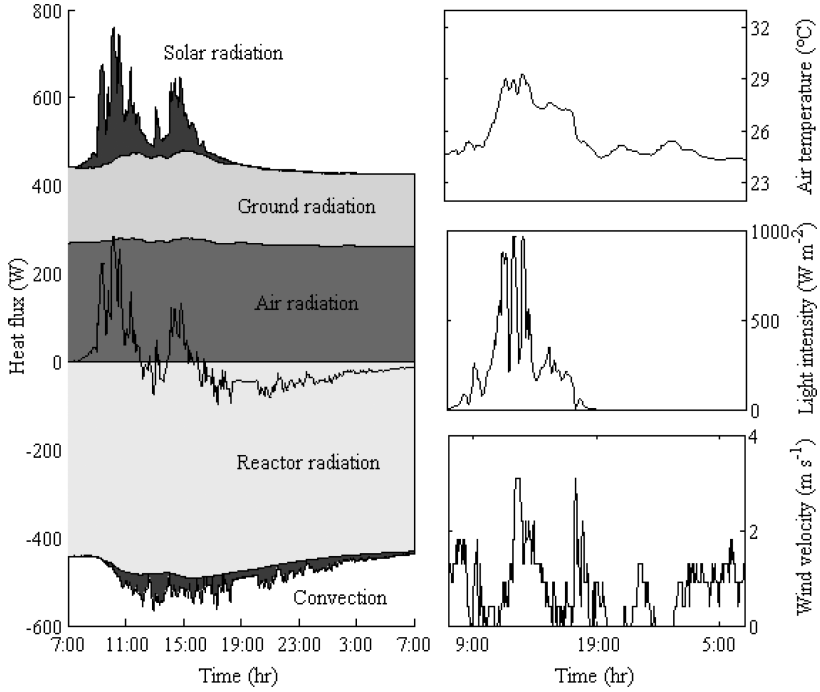

FIGURE 3. Daily changes in heat fluxes reaching a column photobioreactor liquid broth on August 22, 2008, Singapore. The bold plain line represents the total heat flux.

TABLE 1. Sensitivity of Key Parameters

parameter	variation permitted to maintain accuracy of 3 °C	common range (*13, 14*)
fixed		
τ	0.69−0.99	0.7−1.0
r_g	0.02−0.28	0−0.4
K_d	0−0.34	0.1−0.3
$\rho_g Cp_g I_g$	>2 × 10^3 J m^{-2} K^{-1}	2 × 10^5 to 1 × 10^6 J m^{-2} K^{-1}
$T_{g,ref}$	11−27 °C	10−25 °C (generally average air temperature of the year)
$l_{cond,g}$	<0.4 m	0.2−0.5 m
f(t)	±60 min	-
variable		
H_g	±8%	-
v_w	±0.2 m s^{-1}	-
T_a	±0.9 °C	-

perature were mainly due to significant fluctuations in solar radiation (0−200 W) and convective flux (−30 to 50 W), the latter being correlated to the difference between the air and the reactor temperatures. Losses from convection could not compensate the solar heat flux during daytime, which caused temperature to increase. However, convection was the main flux contributing to temperature decrease at night.

On the basis of these observations, a simplified model was constructed using only solar radiation and convection in the heat balance (eq 1) and the model was fitted over the entire set of experimental data. The simplified model was able to predict temperature with an accuracy of 4.7 °C (S10). This approach underestimated cooling at night and the predicted temperature at sunrise of the following day was overestimated by 2 °C. This can be explained by the fact that the difference between the radiation from the surroundings (air and ground) and from the reactor is, although small, not negligible compared to convection at night.

Simulations. Because Singapore may not a particularly suitable location for large-scale algae cultivation due to space requirements, the model was also used to predict temperature changes in a hypothetical column photobioreactor located in Merced, California. Hourly solar irradiance and wind velocity as well as 5-min interval air temperature data were used to feed the model (other parameters are shown in S6). Temperature was simulated over a 1-year period of continuous operation and heat losses caused by periodical introduction of fresh water (to compensate for water evaporation and biomass harvesting) were accounted by introducing the following flux in the heat balance (eq 1):

$$Q_{il/o} = -((1 - RH)X_a F_b + F_h \rho_w) Cp_w (T_r - T_{g,ref}) \quad (32)$$

where F_h is the harvesting rate (10 L day^{-1} $reactor^{-1}$) and with the assumption that freshwater introduced was groundwater at temperature $T_{g,ref}$ (K).

The model predicted temperatures above 35 °C will be achieved during most of the year with peak daily temperatures above 40 °C during the warmest month (Figure 4), a value above the maximum temperature tolerated by most commercial microalgae species.

Modifications to the reactor design were tested and found to have limited impact on temperature changes although both increasing and reducing the reactor radius around 0.1 m were found to slightly reduce the maximum temperatures achieved in the photobioreactor (Figure 5). As the solar flux (in W) is roughly proportional to the reactor lateral surface and the thermal capacity (in J K^{-1}) to the broth volume, a higher reactor radius can indeed result in lower broth temperature. The decrease in peak temperature predicted when reducing the radius to 0.05 m from 0.1 m was therefore surprising but it is explained by to the fact forced convection increases when the radius decreases (eq 27). The reactor radius cannot practically be increased above 0.20 m to avoid the formation of a dark area in the center of the reactor because of intense mutual shading (*18*). An additional simulation showed the use of high-reflectivity ground material (such as concrete of sand) increases the maximum temperatures reached during daytime (S11).

Consequences for Photobioreactor Operation. It is clear from the modeling that broth temperature must be actively controlled in photobioreactors to avoid a significant productivity drop. In the case of a column reactor located in

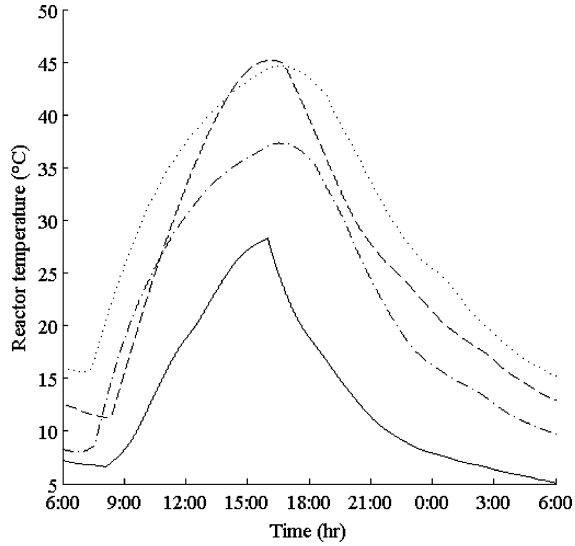

FIGURE 4. Predicted changes from July 23−24, 2009 (dotted line), October 25−26, 2008 (dashed line), January 25−26, 2009 (plain line), and April 25−26, 2009 (dot/dash line) in column photobioreactor broth temperature during outdoor cultivation in July in Merced, California.

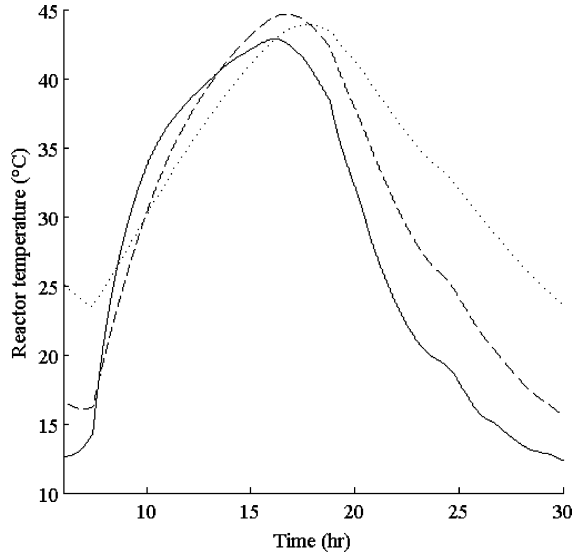

FIGURE 5. Predicted changes in 0.2 m (dotted line), 0.1 m (dashed line), and 0.05 m (plain line) radius column photobioreactor broth temperature during outdoor cultivation in July in Merced, California.

Merced, CA, 18 000 and 5500 GJ year^{-1} ha^{-1} of heat energy must be removed to keep broth temperature at or below 25 and 35 °C, respectively, assuming a density of one reactor per square meter (*19*). This was determined by calculating the energy (J) reaching the reactor during a time step of 1 s and resetting the temperature back to 25 or 35 °C at the end of each time step. The total energy computed over the 5-days data period was then considered representative of each season as shown in Table 2. Temperature control strategies such as water evaporation at the reactor surface or the use of heat exchangers circulating cool water (i.e., deep seawater) have been proposed (*2*). Not even considering cooling efficiency, evaporative cooling would require the distribution and consumption of 2400−8000 m^3 year^{-1} h^{-1} of high-quality groundwater or purified surface water over large arrays of individual photobioreactors (100 000 units for a 10 h production facility delivering, in our example, 365 tonnes of dried algae biomass per year). The use of heat exchangers is no less challenging as it would require significant capital and operation expenditures to supply and distribute cool water. Clearly, temperature control is a major issue that must be addressed when evaluating the technical feasibility, costs, and sustainability of mass algae production in photobioreactors.

TABLE 2. Daily Average Energy (MJ/m^2) Needed to Be Extracted to Maintain the Broth Temperature at T_{max} or Lower in a Column Photobioreactor Operated in Merced, California

season	T_{max} = 25 °C	T_{max} = 35 °C
autumn	4.8	1.6
winter	0.93	0.05
spring	3.0	0.02
summer	11	4.3
year	4.9	1.5

Acknowledgments

We acknowledge ALPHA Biofuels (Singapore), and especially Tan Hai Woon, Chief Technical Officer, for supporting the algae feasibility study that provided experimental data for validation. Dr. Wang Jing-Yuan and Dr. Lim Hock Beng are also gratefully acknowledged for great support at Nanyang Technological University, Singapore. We also thank Miss Qingxia Zhong is for her hard work during the feasibility study and Professor Yusuf Chisti (Massey University) for most valuable discussions on photobioreactors.

Supporting Information Available

S1, schematic representation of the photobioreactor and heat fluxes considered in the heat balance; S2, definition of geometrical parameters; S3, determination of θz and ωs; S4, Tg determination; S5, operation and monitoring of photobioreactor; S6, model input parameters; S7, comparison of predicted vs measured temperature over a 5-d period; S8, discussion of validity of assumptions; S9, temperature prediction using 12 h-averaged meteorological data; S10, temperature prediction using simplified model; S11, influence of ground reflectivity on broth temperature. This information is available free of charge via the Internet at http://pubs.acs.org/.

Literature Cited

(1) Pienkos, P. T.; Darzins, A. The promise and challenges of microalgal-derived biofuels. *Biofuels Bioprod. Biorefining* **2009**, *3* (4), 431–440; DOI 10.1002/bbb.

(2) Chisti, Y. Biodiesel from microalgae beats bioethanol. *Trends Biotechnol.* **2007**, *26* (3), 126–131; DOI 10.1016/j.tibtech.2007.12.002.

(3) Schenk, P. M.; Thomas-Hall, S. R.; Stephens, E.; Marx, U. C.; Mussgnug, J. H.; Posten, C.; Kruse, O.; Hankamer, B. Second Generation Biofuels: High-Efficiency Microalgae for Biodiesel Production. *Bioenergy Resour.* **2008**, *1* (1), 20–43; DOI 10.1007/s12155-008-9008-8.

(4) Dismukes, G. C.; Carrieri, D.; Bennette, N.; Ananyev, G. M.; Posewitz, M. C. Aquatic phototrophs: efficients alternatives to land-based crops for biofuels. *Curr. Opin. Biotechnol.* **2008**, *19* (3), 235–240; DOI 10.1016/j.copbio.2008.05.007.

(5) Packer, M. Algal capture of carbon dioxide; biomass generation as a tool for greenhouse gas mitigation with reference to New Zealand energy strategy and policy. *Energy Policy* **2009**, *37* (9), 3428–3437; DOI 10.1016/j.enpol.2008.12.025.

(6) Lardon, L.; Hélias, A.; Sialve, B.; Steyer, J.-P.; Bernard, O. Life-Cycle Assessment of Biodiesel Production from Microalgae. *Environ. Sci. Technol.* **2009**, *43* (17), 6475–6481; DOI 10.1021/es900705j.

(7) Walker, D. A. Biofuels, facts, fantasy, and feasibility. *J. Appl. Phyco.* **2009**, *21* (5), 509–517; DOI 10.1007/s10911-009-9446-5.

(8) Grobbelaar, J. U. Physiological and technological considerations for optimizing mass algal cultures. *J. Appl. Phyco.* **2000**, *12* (3−5), 201–206.
(9) Ugwu, C. U.; Aoyagi, H.; Uchiyama, H. Photobioreactors for mass cultivation of algae. *Bioresour. Technol.* **2008**, *99* (10), 4021–4028; DOI 10.1016/j.biortech.2007.01.046.
(10) Mata, M. T.; Martins, A. A.; Caetano, N. S. Microalgae for biodiesel production and other applications: A review. *Renew. Sust. Energy Rev.* **2009**, *14* (1), 217–232; DOI 10.1016/j.rser.2009.07.020.
(11) Morita, M.; Watanabe, Y.; Saiki, H. High Photosynthetic Productivity of Green Microalga *Chlorella sorokiniana*. *Appl. Biochem. Biotechnol.* **2000**, *87* (3), 203–218; DOI 10.1385/ABAB:87:3:203.
(12) Chisti, Y. Biodiesel from microalgae. *Biotechnol. Adv.* **2007**, *25* (3), 294–306; DOI 10.1016/j.biotechadv.2007.02.001.
(13) Howell, J. R.; Siegel, R. *Thermal Radiation Heat Transfer*, 4th ed; Taylor & Francis: New York, 2004.
(14) Liu, B. Y. H.; Jordan, R. C. The interrelationship and characteristic distribution of direct, diffuse and total solar radiation. *Sol. Energy* **1960**, *4* (3), 1–19.
(15) Jiji, L. M. *Heat Convection*; Springer: New York, 2006.
(16) Singapore. *National Weather Study Project*; http://nwsp.ntu.edu.sg/weather/new_portal_download_pre.htm.
(17) U.S. National Climatic Data Center Web site; http://www.ncdc.noaa.gov/crn/hourly.
(18) Posten, C. Design principles of photo-bioreactors for cultivation of microalgae. *Eng. Life Sci.* **2009**, *9* (3), 165–177; DOI: 10.1002/elsc.200900003.
(19) Sanchez Miron, A.; Contreras Gomez, A.; Garcia Camacho, F.; Molina Grima, E.; Chisti, Y. Comparative evaluation of compact photobioreactors for large-scale monoculture of microalgae. *J. Biotechnol.* **1999**, *70* (1), 249–270; DOI: 10.1016/S0168-1656(99)00079-6.

ES903214U